2012

Testing a multi-step post-IR IRSL dating method using polymineral fine grains from Chinese loess

Xiao Fu
University of Hong Kong

Bo Li
University of Hong Kong, bli@uow.edu.au

Sheng-Hua Li
University of Hong Kong

Testing a multi-step post-IR IRSL dating method using polymineral fine grains from Chinese loess

Abstract

The potential of multi-elevated-temperature post-IR IRSL (MET-pIRIR) dating [Li, B., Li, S.H., 2011. Luminescence dating of K-feldspar from sediments: a protocol without anomalous fading correction. Quaternary Geochronology 6, 468-479] using polymineral fine grains (FG) (4-11 μm) is tested using loess samples from the Luochuan section in the Chinese Loess Plateau. Nine FG samples with ages within the last glacial-interglacial period are tested using the MET-pIRIR protocol. The MET-pIRIR results for FG are compared with both the coarse grain (63-90 μm) K-feldspar MET-pIRIR dating results and the coarse grain quartz OSL dating results. The stratigraphic age of the profile also provides an independent age control. Our results indicate that the FG MET-pIRIR signals of 200 °C and 250 °C have negligible anomalous fading and they can give reliable ages for the Chinese loess within the last glacial-interglacial period.

Keywords

ir, irsl, dating, method, polymineral, fine, testing, grains, multi, chinese, loess, step, post, CAS

Disciplines

Life Sciences | Physical Sciences and Mathematics | Social and Behavioral Sciences

Publication Details

Fu, X., Li, B. & Li, S. (2012). Testing a multi-step post-IR IRSL dating method using polymineral fine grains from Chinese loess. Quaternary Geochronology, 10 8-15.

Testing a multi-step post-IR IRSL dating method using polymineral fine grains from Chinese loess

Xiao Fu, Bo Li, Sheng-Hua Li**Department of Earth Sciences, The University of Hong Kong, Pokfulam Road, Hong Kong, China*

**Corresponding author: shli@hku.hk*

Abstract: The potential of multi-elevated-temperature post-IR IRSL (MET-pIRIR) dating (Li and Li, 2011) using polymineral fine grains (FG) (4-11 μm) is tested using loess samples from the Luochuan section in the Chinese Loess Plateau. Nine FG samples with ages within the last glacial-interglacial period are tested using the MET-pIRIR protocol. The MET-pIRIR results for FG are compared with both the coarse grain (63-90 μm) K-feldspar MET-pIRIR dating results and the coarse grain quartz OSL dating results. The stratigraphic age of the profile also provides an independent age control. Our results indicate that the FG MET-pIRIR signals of 200 °C and 250 °C have negligible anomalous fading and they can give reliable ages for the Chinese loess within the last glacial-interglacial period.

Key words: feldspar, MET-pIRIR protocol, Chinese loess, fine grain

1. Introduction

In north China, loess deposits are widely distributed. Important information about Quaternary climate changes is preserved in these sediments, however, its significance can only be explored on the basis of reliable chronology research. The broad age framework of Chinese Loess on a glacial/interglacial time-scale has been well established by correlating its straitigraphy and climate records to deep sea records (e.g. Liu, 1985; Porter and An, 1995; Liu et al., 2000; Ding et al., 2002), and so new dating techniques can be tested using Chinese loess.

Optically stimulated luminescence (OSL) dating plays an important role in providing a chronology for loess on a shorter time-scale within the last glacial-interglacial period (Lu et al., 2007; Lai, 2010; Roberts, 2008). In OSL dating, both quartz and feldspar can be used as a palaeodosimeter (Aitken, 1998). Since the development of the single aliquot regeneration (SAR) technique (Murray and Wintle,

2000), quartz is usually taken as the preferred choice for dating of sediments. However, early saturation in the dose response curve (DRC) for quartz OSL signal limits its application for dating old samples. Compared with the quartz OSL signal, the infrared stimulated luminescence (IRSL) signal (Hütt et al., 1988) from feldspar appears to saturate at a higher dose. Thus, it has a great potential for extending the OSL dating range. Unfortunately, the application of IRSL dating has long been hampered by the phenomenon of anomalous fading (Wintle, 1973; Huntley and Lamothe, 2001). In recent years, advances related to overcome the anomalous fading problem have been achieved. These include the methods for fading correction (Huntley and Lamothe, 2001; Kars et al., 2008), and the protocols for extracting non-fading components (Li et al, 2008; Tsukamoto et al., 2006; Thomsen et al., 2008; Buylaert et al., 2009; Thiel et al., 2011; Li and Li, 2011). Thomsen et al. (2008) reported that a post-IR IRSL signal obtained using an elevated temperature IR stimulation following the low temperature IR stimulation has a lower fading rate compared with conventional IRSL. Consequently, the two-step post-IR IRSL signal has been used by Buylert et al. (2009) for dating coarse-grain K-feldspar (CG KF) and Thiel et al. (2011) for dating polymineral fine-grain (FG) extracts. However, there is still a detectable anomalous fading (~1-2%) in the two-step post-IR IRSL signal (Buylert et al., 2009), although Thiel et al. (2011) argued that there is no need to make allowance for such a small fading rate for their samples.

Recently, a multi-elevated-temperature post-IR IRSL protocol (MET-pIRIR) for optical dating of KF has been proposed by Li and Li (2011). In this protocol, a multi-step of IRSL measurements with increasing stimulation temperature from 50 to 250°C were conducted to obtain a series of MET-pIRIR signals, and thus, their corresponding D_e values and ages. At high simulation temperatures of 200 and 250°C, the MET-pIRIR ages were similar and suggested that signals with negligible anomalous fading have been achieved. The advantage of this method over the two-step post-IR IRSL method is that the appearance of such an age plateau serves as an indicator that real non-fading signals have been obtained, and there is negligible anomalous fading (<1%/decades) for the MET-pIRIR signals above 200 °C (Li and Li, 2011).

In this study, we aim to test the potential of MET-pIRIR dating using FG (4-11 μm) polymineral from loess. Samples were collected from the well known Luochuan section on the Chinese Loess Plateau,

which located in the Shaanxi province, China (e.g. Liu, 1985; An et al., 1990, 1991; Porter and An, 1995; Xiao et al., 1995). Detailed quartz OSL ages within the last 130 ka for the section have been reported (Buylert et al., 2007; Lu et al., 2007; Lai, 2010). The stratigraphic ages of the profile also provides an independent age control. The advantage of using FG is that this is the dominant grain size of the minerals in Chinese loess, and there is a negligible contribution from the internal dose rate, hence there is no need to assume the concentrations of internal radioactive elements (^{40}K and ^{87}Rb).

2. Samples and facilities

In this study, we collected a series of samples from the upper part of the Luochuan section, including one sample from the Holocene soil unit S0 (corresponding to the Marine Isotope Stage (MIS) 1), seven samples from the Last Glacial loess unit L1 (corresponding to MIS 2-4) and 1 sample from the Last Interglacial paleosol unit S1 (corresponding to MIS 5), which are all within the quartz OSL dating limit (Lu et al., 2007; Lai, 2010), to test the reliability of the FG MET-pIRIR dating method.

All samples were collected by hammering stainless steel tubes into the cleaned section. In the dark room, samples were treated under subdued red light. 2-cm-thick outer layers of the samples were removed and used for dose rate measurement, 30% H_2O_2 and 10% HCl were used to remove organic matter and carbonates, respectively. FG (4-11 μm) fractions were isolated using a settlement technique similar to Zhang and Zhou (2007) and Fu et al. (2010). CG (63-90 μm) KF and CG quartz were also obtained by wet sieving and heavy liquid separation (Li et al., 2008). Etching with 10% and 40% HF for 40 mins were carried out for CG KF and CG quartz extracts, respectively. The IR depletion ratio (Duller, 2003) was used for checking the purity of quartz fractions.

All luminescence measurements were performed using an automated Risø TL/OSL-DA-20 reader equipped with a ^{90}Sr/^{90}Y beta source. IR diode (870±40 nm) and blue diode (470±30 nm) were used for IR and blue-light stimulation, respectively. Luminescence was detected by an EMI 9235QA photomultiplier tube. When measuring the MET-pIRIR signals (for both FG polyminerals and CG KF), a filter pack of Schott BG-39 and Corning 7-59 filters was equipped in front of the PMT. When measuring the quartz OSL signal, three 2.5 mm Hoya U-340 filters were used. The measurement time of all optical signals is 100 s. For FG MET-pIRIR measurement, the first 5 s integral of the initial

decay curves minus backgrounds estimated from the last 5 s integral were used for D_e calculation. For CG KF MET-pIRIR and quartz OSL measurements, the first 2 s integral of the initial decay curves minus backgrounds estimated from the last 5 s integral were used for D_e calculation. For the dose recovery experiments, an ORIEL solar simulator was used for bleaching the natural signals.

For annual dose evaluation, the contents of U, Th were measured using the thick-source alpha counting technique (Aitken, 1985), and the content of K was evaluated using X-ray fluorescence. Water content was assumed to be 15±5% for loess and 20±5% for paleosol, based on the measurement results reported by previous studies (Lu et al., 2007). Cosmic-ray dose rate was calculated following Prescott and Hutton (1994). For FG, the alpha efficiency was assumed to be 0.08±0.02 (Rees-Jones, 1995). For CG KF, the internal K and Rb contents were assumed to be 13±1% and 400±100 ppm, respectively (Huntley and Baril, 1997; Zhao and Li, 2005; Li et al., 2008).

3. Luminescence properties of the MET-pIRIR signals

The MET-pIRIR procedure for FG used in this study is listed in Table 1, and is similar to that used for CG KF (Li and Li, 2011). In this protocol, preheating of 300°C for 10 s was used, and then five steps of IRSL measurements with simulation temperature increasing from 50°C to 250°C were conducted. Signals from test doses were used for correcting the sensitivity changes. The sensitivity-corrected signals ($L_x(T)/T_x(T)$) were used to construct the dose response curves and estimate equivalent doses for the MET-pIRIR signals. It should be noted that before all the measurements, the aliquots were held at the measurement temperature for 5 s without IR stimulation to test the intensity of the residual isothermal TL (ITL) after preheating.

Luminescence properties of the FG extracts were investigated using the sample LC-045 with a quartz OSL age of ~34 ka. Fig. 1a shows typical MET-pIRIR decay curves with increased stimulation temperatures for this sample. It is observed that after the preheating of 300°C for 10 s, the high temperature MET-pIRIR signals are usually less than one tenth of the 50°C IRSL signal. Considering that the signal intensity of FG is relatively low (usually thousands of counts for the natural 50°C IRSL), in order to ensure sufficient intensity of the MET-pIRIR signals, stringent preheating should be

avoided.

A pulse annealing experiment (Duller, 1994; Li et al., 1997) was used to investigate the thermal stability difference between the FG and the CG KF from sample LC-045. In this experiment, after bleaching the natural signal, the aliquot was given a regeneration dose of 18 Gy, cut-heat to 200°C, and the IRSL signal was measured. After that, a test dose of 18 Gy was given, followed by a cut-heat to 200°C and then the test dose IRSL signal was measured. The test dose signal is used to monitor the sensitivity change. Such measurement cycles are repeated, with 20°C increments in the cut-heat temperature for the regeneration dose, while the cut-heat temperature remains fixed for the test dose. A 'hot' IR bleaching at 320°C for 100s was applied after each cycle to erase the residual signals. All the heating treatments in the experiment were performed with a heating rate of 5°C /s. The pulse annealing results are shown in Fig.1b. The IRSL from FG decrease earlier than that from CG KF. After heating to 300°C, the remaining IRSL signal from CG KF is ~75%, while the remaining IRSL signal from FG is less than 50%. Because different grain sizes are compared here, a possible lag in heating to CG compared with FG may probably cause difference in their pulse annealing curves. However, Li and Wintle (1992) showed that under a heating rate of 5°C /s, pulse annealing curves of FG KF and CG KF are nearly identical. The significant difference in Fig. 1b. was not related to the difference in thermal lags of different grain sizes. Hence, the pulse annealing results demonstrate that IRSL from FG is less thermally stable than CG KF. Li and Wintle (1992) and Li et al. (2011) suggested that the IRSL signal from Na-feldspar (NaF) uses a higher proportion of shallow traps than that from KF. Therefore, such distinct difference in thermal stabilities between CG KF and FG polymineral suggests that a significant part of the IRSL signal from FG polymineral is originated from NaF.

Fig. 1c shows different dose response curves obtained using different MET-pIRIR signals. The dose response curves (DRCs) can be fitted using single exponential saturation functions. Higher stimulation temperatures result in earlier saturation of the DRC was observed. The saturation doses (D_0) are 282, 252, 270, 253 and 223 Gy for the 50, 100, 150, 200 and 250 °C signals, respectively. This tendency is also similar to that observed for CG KF (Li and Li, 2011).

The recycling ratios and recuperation were checked when constructing the DRCs. For all the samples in

this study, the recycling ratios of all signals are within 1.0 ± 0.1, indicating an effective sensitivity correction. The magnitude of recuperation is dependent on the sample age and the stimulation temperature. The recuperation of younger samples is usually larger than that for older samples, and the recuperation increases with the measurement temperatures. For our samples, the recuperations of MET-pIRIR signals of 50, 100 and 150°C are generally less than 5% of the natural signals, and the recuperations of MET-pIRIR signals of 200 and 250°C are generally less than 10%, except for the youngest sample LC-004 (~0.7 ka), in which the recuperation reaches as high as ~50% for the MET-pIRIR signal of 250°C. For sample LC-004, the high recuperation value compared to the weak natural signals suggests that the D_e values obtained for this sample are an apparent result of residual dose and thermal transfer, and it is difficult to accurately determine the effect of thermal transfer on D_e values. However, if the zero-dose point is projected onto the DRCs by forcing the curves to the origin, a recuperation dose of ~ 2.4 Gy was obtained for the 250°C MET-pIRIR signals. Such value is negligible for older samples with much higher natural doses, but significant for younger sample, like LC-004.

To test the suitability of the protocol, a dose recovery test was also conducted on LC-045. Six aliquots were bleached under the solar simulator for 1.5 hours, and then divided into two groups: Group 1 (two aliquots) was measured immediately using procedures in Table 1 to measure the residual dose. Group 2 (four aliquots) was given a beta dose of 115 Gy, which is similar to the expected D_e. They were then stored in dark at room temperature for a week which allows for fading. After the storage, the given dose was measured using the procedure in Table 1. The residual dose measured from Group 1 is 2.0 ± 0.1 Gy, 3.2 ± 0.1 Gy, 3.6 ± 0.2 Gy, 4.2 ± 0.7 Gy, 5.5 ± 1.1 Gy for the MET-pIRIR signals at 50°C, 100°C, 150°C, 200°C and 250°C, respectively. For typical dose rate of 3 Gy/ka, these residual doses are equal to 1-2 ka. It is similar to the results of Li and Li (2011) for CG, and indicates that compared with signals with lower stimulation temperature, signals obtained with higher temperature are harder to be bleached. The dose recovery results from Group 2 show that after subtraction of the residual dose measured from Group 1, the recovered doses are 104 ± 2 Gy, 106 ± 3 Gy, 109 ± 4 Gy, 111 ± 3 Gy and 111 ± 4 Gy for the MET-pIRIR signals at 50°C, 100°C, 150°C, 200°C and 250°C, respectively. The increasing measured dose with temperature indicates that signals with less fading are obtained at higher stimulation temperature, thus no further fading test for these signals is needed.

The recovered doses for the MET-pIRIR signals at 200°C and 250°C are in good agreement with the given dose, indicating that the procedures in Table 1 work well with our sample.

4. Dating results and discussions

The applicability of the protocol in Table 1 was examined on nine samples collected from S0, L1 and S1. For comparison, the CG KF MET-pIRIR ages for all samples were obtained using the method of Li and Li (2011), and the quartz OSL ages for some samples were also obtained by dating CG quartz extracts using the SAR method (Murray and Wintle, 2000). All ages are summarized in Table 2.

Using the MET-pIRIR protocol, five D_e values are produced. A plot of age versus temperature (A-T plot) can be observed. The appearance of an age plateau is assumed to indicate that a non-fading signal has been achieved. Fig. 2 shows typical A-T plots from four samples. It is shown that the MET-pIRIR ages increase with stimulation temperature from 50 to 200°C. The quartz ages of those samples are also shown as gray belts in the figures for comparison. Except the youngest sample (LC-004 in Fig 2a), , the 50 and 100°C ages are all underestimated (Fig. 2b, c and d), but there is a lower underestimation for higher stimulation temperature, suggesting a lower anomalous fading rate for the signals at higher temperatures. The 200 and 250 °C ages for all samples reach an age plateau, which is expected for the MET-pIRIR method (Li and Li, 2011). The 200 and 250 °C ages are also consistent with the quartz ages, indicating that non-fading signals were obtained. The results in Fig. 2 imply that the MET-pIRIR signals of 200 and 250°C can be used to date FG polyminerals from loess samples up to 75 ka without using a fading correction.

For the S0 sample LC-004 (Fig. 2a), the MET-pIRIR age keeps increasing from 50°C to 250°C, and no plateau in age can be observed. Compared with the quartz OSL age of ~0.7 ka, all MET-pIRIR ages are overestimated, ages from ~ 1 ka for the 50°C signal to ~ 1.9 ka for the 250°C signal. Such discrepancy can be explained as a result of thermal transfer and residual signals. Such residual ages are consistent with our results after bleaching (the last section) and previous reports (Li, 1994; Li and Li, 2011), which suggest that the IRSL and MET-pIRIR signals have a residual age ranging from several hundred years to a few thousand years, with higher residual ages at higher stimulation

temperatures. The problem of age overestimation caused by the residual signals and the high recuperation for LC-004 indicates that cautions should be taken when dating young samples of hundreds of years to several thousand years using the MET-pIRIR protocol. However, such residual age of 2 ka will not significantly affect the dating results for old samples, say, 50 ka.

Since the signals of FG are relatively weak, it is not practical to use a strong preheating due to thermal erosion. However, a potential problem of using a moderate preheating is that when measuring the high temperature MET-pIRIR signal (mainly for the highest temperature 250 °C, which is closest to the preheating temperature), there may be a significant interference from the residual TL. This can be monitored by holding the sample at the measurement temperature for 5 s before IR stimulation. For most of our samples, it is found that a preheating of 300°C for 10 s is sufficient to reduce the residual ITL intensity to a negligible level, even for the highest IR stimulation temperature (see example of the 250°C signal of LC-054 in Fig. 3a). However, two samples, LC-065 and LC-082, were exceptions. Fig. 3b shows the natural 250°C MET-pIRIR signal with the 5 s of IR-off time for sample LC-082. The residual ITL signal was strong, which are comparable to the measured "MET-pIRIR signal", indicating an inadequate preheating. Such effect of the large residual ITL signal can be seen in the A-T plots in Fig. 4a and b. The ages increase with the stimulation temperatures from 50 to 200°C, and the ages decrease to the lowest level at 250°C. In order to solve this problem, we extended the duration of the IR-off time from 5 s to 100 s before the 250°C MET-pIRIR measurements for these samples. A natural decay curve of the 250°C MET-pIRIR signal with 100-s IR-off time for LC-082 is shown in Fig. 3c. The 100 s delay at 250°C reduces the intensity of the residual ITL signal to a level lower than the later part of the decay curve when the IR stimulation was on. Therefore, we modified the dating procedures for these two samples by increasing the IR-off time to 100 s for step 7 and 14 in Table 1. The dating results utilizing the modified protocol are present in Fig. 4 a and b. Using the improved protocol, an age plateau can be reached for the 200 and 250°C signals. The ages obtained are all consistent with the quartz ages.

Fig. 5a presents the stratigraphy of the section and the FG MET-pIRIR dating results for all the samples. A gradual increase in MET-pIRIR ages from low stimulation temperature to high stimulation temperature is observed for all the samples. Fig. 2 and 5a both show that the 200 and 250°C ages are

consistent with each other except for the youngest sample LC-004. The FG MET-pIRIR dating results together with the CG KF MET-pIRIR dating results and the quartz ages are summarized in Fig. 5b. The three ages are also compared in Fig. 6. Except for the modern sample LC-004, the three ages are in good agreement with each other, confirming that the using the MET-pIRIR protocol, non-fading signals can be obtained from the FG extracts.

The stratigraphy of the section also provides an age control for the samples. Two samples LC-015 and LC-093, which were collected from the boundaries of S0/L1 and L1/S1, give ages of 13.8 ± 1.1 ka and 75.1 ± 7.9 ka using the 250 °C MET-pIRIR signal, respectively. They are consistent with the MIS 1/2 and MIS 4/5 transition ages of 12.05 ka and 73.91 ka (Martinson et al. 1987; Porter and An, 1995).

The gross deposition rate for L1 is calculated to be 13.3 ± 1.0 cm/ka (Fig. 5b) by regressing the FG MET-pIRIR ages with the sample depths. This is similar to the result of 15.2 cm/ka obtained by Lai (2010).

5. Conclusions

The potential of MET-pIRIR dating using fine grain polymineral is tested using the Chinese loess samples from the Luochuan section. For samples within the last glacial-interglacial period, the 200 and 250°C MET-pIRIR ages are consistent with the CG KF MET-pIRIR ages, quartz OSL ages and stratigraphic ages. Our results indicate that the MET pIRIR signals of 200 °C and 250 °C for FG have negligible anomalous fading and give reliable ages for the Chinese loess. However, cautions must be taken when dating samples as young as a few hundreds of years using the MET-pIRIR protocol, because of the relatively high residual age and recuperation. Dating using FG polyminerals has an advantage over CG KF since no internal dose was involved.

Acknowledge

We thank X.L. Wang and Y.W. Chen for their help in sample collection. S. Lowick is appreciated for reviewing the paper and providing valuable comments on it. This study was financially supported by

the grants to SHL from the Research Grant Council of the Hong Kong Special Administrative Region, China (Project no. 7035/07P and 7028/08P).

Reference

Aitken, M.J., 1985. Thermoluminescence dating. Academic Press, London.

Aitken, M.J., 1998. An introduction to luminescence dating. Oxford University Press, London.

An, Z.S., Kukla, G.J., Porter, S.C., Xiao, J., 1991. Magnetic susceptibility evidence of monsoon variation on the Loess Plateau of central China during the last 130,000 years. Quaternary Research 36, 29-36.

An, Z.S., Liu, T.S., Lu, Y.C., Porter, S.C., Kukla, G., Wu, X.H., Hua, Y.M.,1990. The long term paleomonsoon variation recorded by the loess-paleosol sequence in central China. Quaternary International 7/8, 91-95.

Buylaert, J.P., Murray, A.S., Thomsen, K., Jain, M., 2009.Testing the potential of an elevated temperature IRSL signal from K-feldspar. Radiation Measurements 44, 560-565.

Buylaert, J.P., Vandenberghe, D., Murray, A.S., Huot, S., De Corte, F., Van den Haute, P., 2007. Luminescence dating of old (>7 ka) Chinese loess: a comparison of single-aliquot OSL and IRSL techniques. Quaternary Geochronology 2, 9-14.

Ding, Z. L., Derbyshire, E., Yang, S. L., Yu, Z. W., Xiong, S. F., Liu, T. S., 2002. Stacked 2.6-Ma grain size record from the Chinese loess based on five sections and correlation with the deep-sea $\delta^{18}O$ record. Paleoceanography 17, NO. 3, 1033. 10.1029/2001PA000725.

Duller, G.A.T., 1994.A new method for the analysis of infrared stimulated luminescence data from potassium feldspars. Radiation Measurements 23, 281-285.

Duller, G.A.T., 2003. Distinguishing quartz and feldspar in single grain luminescence measurements. Radiation Measurements 37, 161-165.

Fu. X., Zhang, J.F., Mo, D.W., Shi, C.X., Liu, H., Li, Y.Y., Zhou, L.P., 2010. Luminescence dating of baked earth and sediments from the Qujialing archaeological site, China. Quaternary Geochronology 5, 353-359.

Huntley, D.J., Baril, M.R., 1997. The K content of the K-feldspars being measured in optical dating or in thermoluminescence dating. Ancient TL 15, 11-13.

Huntley, D. J., Lamothe, M., 2001. Ubiquity of anomalous fading in K-feldspars and the measurement and correction for it in optical dating. Canadian Journal of Earth Sciences 38, 1093-1106.

Hütt, G., Jaek, I., Tchonka, J., 1988. Optical dating: K-feldspar optical response stimulation spectra. Quaternary Science Reviews 7, 381-385.

Kars, R.H., Wallinga, J., Cohen, K.M., 2008. A new approach towards anomalous fading correction for feldspar IRSL dating-tests on samples in field saturation. Radiation Measurements 43, 786-790.

Lai, Z.P., 2010. Chronology and the upper dating limit for loess samples from Luochuan section in the Chinese Loess Plateau using quartz OSL SAR protocol. Journal of Asian Earth Sciences 37, 176-185.

Li, B., Li, S.H., Wintle, A.G., Zhao, H., 2008. Isochron dating of sediments using luminescence of K-feldspar grains. Journal of Geophysical Research-Earth Surface 113, F02026, doi :02010.01029 / 02007JF000900.

Li, B., Li, S.H., 2011. Luminescence dating of K-feldspar from sediments: A protocol without anomalous fading correction. Quaternary Geochronology 6, 468-479.Li, B., Li, S.H., Duller, G.A.T., Wintle, A.G., 2011. Infrared stimulated luminescence measurements of single grains of K-rich feldspar for isochron dating. Quaternary Geochronology 6, 71-81.

Li, S.H., 1994. Optical dating: Insufficiently bleached sediments. Radiation Measurements 23, 563-567.

Li, S.H., Tso, M.Y.W., Wong, N.W.L., 1997. Parameters of OSL traps determined with various linear heating rates. Radiation Measurements 27, 43-47.

Li, S.H., Wintle, A.G., 1992. A global view of the stability of luminescence signals from loess. Quaternary Science Reviews 11, 133-137.

Liu, T.S. (Ed.), 1985. Loess and the Environment. China Ocean Press, Beijing.

Liu, T. S., Ding, Z. L., Rutter, N. W., 2000. Comparison of Milankovitch periods between continental loess and deep sea records over the last 2.5 Ma. Quaternary Science Reviews, 18, 1205-1212.

Lu, Y.C., Wang, X.L, Wintle, A.G., 2007. A new OSL chronology for dust accumulation in the last 130,000 yr for the Chinese Loess Plateau. Quaternary Research 67, 152-160.

Martinson, D.G., Pisias, N.G., Hays, J.D., Imbrie, J., Moore, T.C., Shackleton, N.J., 1987. Age dating and the orbital theory of the ice ages: Development of a high-resolution 0 to 300,000 year chronostratigraphy. Quaternary Research 27, 1-29.

Murray, A.S., Wintle, A.G., 2000. Luminescence dating of quartz using an improved single-aliquot regenerative-dose protocol. Radiation Measurements 32, 57-73.

Porter, S.C., An, Z.S., 1995. Correlation between climate events in the North Atlantic and China during the last glaciation. Nature 375, 305-308.

Prescott, J.R., Hutton, J.T., 1994. Cosmic ray contributions to dose rates for luminescence and ESR dating: large depths and long-term time variations. Radiation Measurements 23, 497-500.

Rees-Jones, J., 1995. Optical dating of young sediments using fine-grain quartz. Ancient TL 13, 9-14.

Roberts, H.M., 2008. The development and application of luminescence dating to loess deposits: a perspective on the past, present and future. Boreas 37, 483-507.

Thiel, C.,Buylaert, J.P., Murray, A.S., Terhorst, B., Hofer, I., Tsukamoto, S., Frechen, M., 2011. Luminescence dating of the Stratzing loess profile (Austria) - testing the potential of an elevated temperature post-IR IRSL protocol. Quaternary International 234, 23-31.

Thomsen, K.J., Murray, A.S., Jain, M., Bøtter-Jensen, L., 2008. Laboratory fading rates of various luminescence signals from feldspar-rich sediment extracts. Radiation Measurements 43, 1474-1486.

Tsukamoto, S., Denby, P.M., Murray, A.S., Bøtter-Jensen, L., 2006. Time-resolved luminescence from feldspars: New insight into fading. Radiation Measurements 41, 790-795.

Wintle, A.G., 1973. Anomalous fading of thermoluminescence in mineral samples. Nature 245, 143-144.

Xiao, J.L., Porter, S.C., An, Z.S., Kumai, H., Yoshikawa, S., 1995. Grain-Size of quartz as an indicator of winter monsoon Strength on the loess plateau of central China during the last 130,000-Yr. Quaternary Research 43, 22-29.

Zhang, J.F., Zhou, L.P., 2007. Optimization of the 'double SAR' procedure for polymineral fine grains. Radiation Measurements 42, 1475-1482.

Zhao, H., Li, S.H., 2005. Internal dose rate to K-feldspar grains from radioactive elements other than potassium. Radiation Measurements 40, 84-93.

Caption

Fig. 1. Luminescence characters of the FG extracts. All the measurements were carried out on a typical sample LC-045. a) Decay curves for the MET-pIRIR signals obtained at different stimulation temperatures. All data are normalized to the first point of the 50°C signal. b) Pulse annealing results for CG KF and FG extracts. All data are normalized to the first data point of 200°C. c) DRCs for the MET-pIRIR signals. A saturating exponential function was used for fitting.

Fig. 2. Typical A-T plots from four samples with different ages. The gray belts in the plots are quartz ages for these samples.

Fig. 3. a) The natural decay curve for the 250°C MET-pIRIR signal of sample LC-054. The IR-off time is 5 s. b) & c) The natural decay curve for the 250°C MET-pIRIR signal of sample LC-082. The IR-off times are 5 s and 100 s, respectively. In all figures, the red lines indicate the backgrounds, the gray belts indicate the ITL signals in the IR-off period.

Fig. 4. A-T plots for a) LC-065 and b) LC-082 with different IR-off time before measurements of the 250°C MET-pIRIR signals. The gray belts are quartz ages for the samples.

Fig. 5. Summary of the FG MET-pIRIR dating results for samples within the last glacial-interglacial cycle. a) The stratigraphy and all the FG MET-pIRIR dating results. b) The stratigraphy and summary of the FG MET-pIRIR, CG KF MET-pIRIR and quartz OSL ages. For both FG and CG KF, the 250°C MET-pIRIR ages are selected as the final dating results. For samples LC-015 and LC-026, because lack of sufficient CG quartz for dating, we did not obtain corresponding quartz OSL ages. For LC-015, which is located at the transition belt of L1 and S0, its age is expected to be 12.05 ka based on previous studies (Martinson et al. 1987; Porter and An, 1995). The quartz age of 11.7±0.4 obtained by Lu et al. (2007) for this transition is also consistent with expected age. For LC-026, we used the quartz OSL age of 28.0 ± 1.3 ka from Lu et al. (2007). The red dashed line represents the regression line between the FG MET-pIRIR age and the depth for samples within L1. The insets in both figures show the details of sample LC-004 and LC-015.

Fig. 6. Comparison of the FG MET-pIRIR dating results and a) the quartz OSL dating results; b) the CG KF MET-pIRIR dating results. All data are from Fig. 5.

Table 1 The MET-pIRIR protocol for FG

Step	Treatment	Observed
1	Give regenerative dose, D_i	
2	Preheat at 300°C for 10 s	
3	IRSL measurement at 50°C for 100 s	$\mathbf{L_{x(50)}}$
4	IRSL measurement at 100°C for 100 s	$\mathbf{L_{x(100)}}$
5	IRSL measurement at 150°C for 100 s	$\mathbf{L_{x(150)}}$
6	IRSL measurement at 200°C for 100 s	$\mathbf{L_{x(200)}}$
7	IRSL measurement at 250°C for 100 s	$\mathbf{L_{x(250)}}$
8	Give test dose, D_t	
9	Preheat at 300°C for 10 s	
10	IRSL measurement at 50°C for 100 s	$\mathbf{T_{x(50)}}$
11	IRSL measurement at 100°C for 100 s	$\mathbf{T_{x(100)}}$
12	IRSL measurement at 150°C for 100 s	$\mathbf{T_{x(150)}}$
13	IRSL measurement at 200°C for 100 s	$\mathbf{T_{x(200)}}$
14	IRSL measurement at 250°C for 100 s	$\mathbf{T_{x(250)}}$
15	IR bleaching at 320°C for 40 s	
	Return to step1	

Note: For the first cycle natural signals were recorded. The later five regeneration cycles include a zero dose D_4=0 and two repeated regenerative doses D_1=D_5.

Table 2 Summary of the dating results

Sample	Depth, m	Unit	K content,%	α counting, cts	Water content, %	FG dose rate, Gy/ka	FG MET-pIRIR De, Gy					FG MET-pIRIR age, ka					CG KF MET -pIRIR age. ka	Quartz OSL age, ka
							50°C	100°C	150°C	200°C	250°C	50°C	100°C	150°C	200°C	250°C		
LC-004	0.4	S0	1.86	13.5±0.2	20±5	3.5±0.2	3.47±0.09	4.37±0.66	4.98±0.5	5.79±0.65	6.53±0.75	0.99±0.07	1.24±0.20	1.42±0.17	1.65±0.21	1.86±0.25	1.48±0.14	0.65±0.08
LC-015	1.5	L1	1.91	12.5±0.2	15±5	3.6±0.3	36.2±1.5	40.5±0.6	45.3±0.9	47.5±1.7	49.2±2.1	10.2±0.8	11.4±0.8	12.7±0.9	13.3±1.1	13.8±1.1	14.2±0.9	
LC-026	2.6	L1	1.81	10.7±0.2	15±5	3.2±0.2	63.5±5.8	71.1±4.4	78.4±1.2	82.2±4.1	87.5±6.7	19.9±2.3	22.3±2.1	24.5±1.8	25.7±2.2	27.4±2.9	23.5±1.6	28.0±1.3[#]
LC-035	3.5	L1	1.95	11.5±0.2	15±5	3.4±0.2	76.5±1.5	85.8±1.2	95.1±1.0	99.2±1.1	102.9±1.9	22.5±1.7	25.2±1.8	27.9±2.0	29.1±2.1	30.2±2.2	27.2±1.7	31.4±4.2
LC-045	4.5	L1	1.96	12.0±0.2	15±5	3.5±0.3	93.1±2.5	105.7±1.7	113.2±1.2	120.7±2.3	120.9±3.2	26.8±2.1	30.4±2.2	32.6±2.4	34.7±2.6	34.8±2.7	33.9±2.2	34.6±1.8
LC-054	5.4	L1	1.98	12.3±0.2	15±5	3.5±0.3	107.9±1.7	125.2±2.3	140.6±1.5	151.6±2.6	145.1±3.4	30.6±2.3	35.5±2.6	39.9±2.9	43±3.2	41.2±3.1	42.4±2.8	46.3±4.2
LC-065	6.5	L1	2.02	12.4±0.2	15±5	3.6±0.3	139.6±5.7	148.8±1.6	153.3±3.2	186.1±5.4	184.9±10.0	39.1±3.2	41.7±3.3	43±3.2	52.2±4.1	51.8±4.7	51.4±3.8	51.2±3.3
LC-082	8.2	L1	1.84	11.5±0.2	15±5	3.3±0.2	166.3±5.0	177.1±2.3	205.9±3.8	223.3±8.5	217.6±13.0	50.8±4.0	54.1±4.0	62.9±4.7	68.2±5.6	66.5±6.2	66.1±3.9	62.3±6.8
LC-093	9.3	S1	1.9	10.5±0.2	20±5	3.0±0.2	172.1±4.5	191.6±5.9	220.8±3.4	228.1±6.7	226.9±17.7	57.0±4.2	63.4±4.8	73.1±5.2	75.5±5.7	75.1±7.9	74.8±4.2*	73.8±5.7

*Data cited from Li and Li (2011);

Data cited from Lu et al. (2007). See details in Fig. 5.' caption.

1 Fig. 1

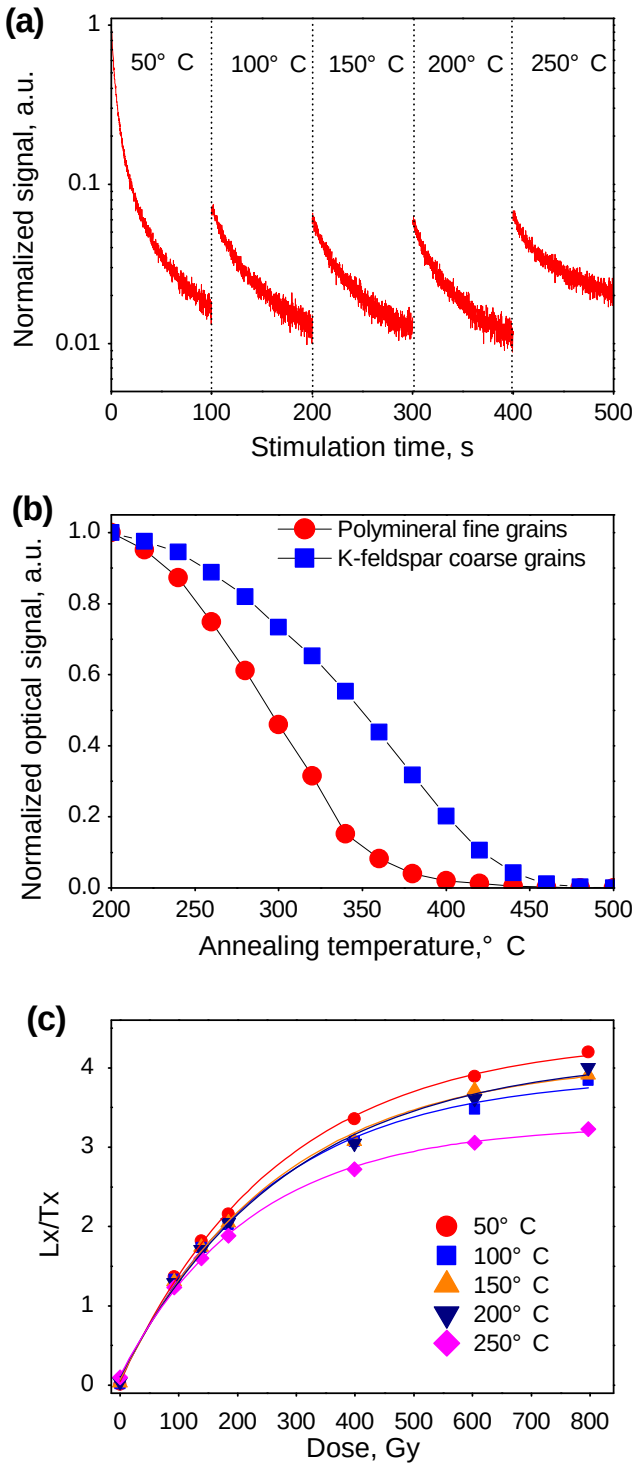
(a)
50° C
100° C
150° C
200° C
250° C
Normalized signal, a.u.
1
0.1
0.01
0
100
200
300
400
500
Stimulation time, s
(b)
Polymineral fine grains
K-feldspar coarse grains
Normalized optical signal, a.u.
1.0
0.8
0.6
0.4
0.2
0.0
200
250
300
350
400
450
500
Annealing temperature,° C
(c)
Lx/Tx
4
3
2
1
0
50° C
100° C
150° C
200° C
250° C
0
100
200
300
400
500
600
700
800
Dose, Gy

2

3

1 Fig. 2

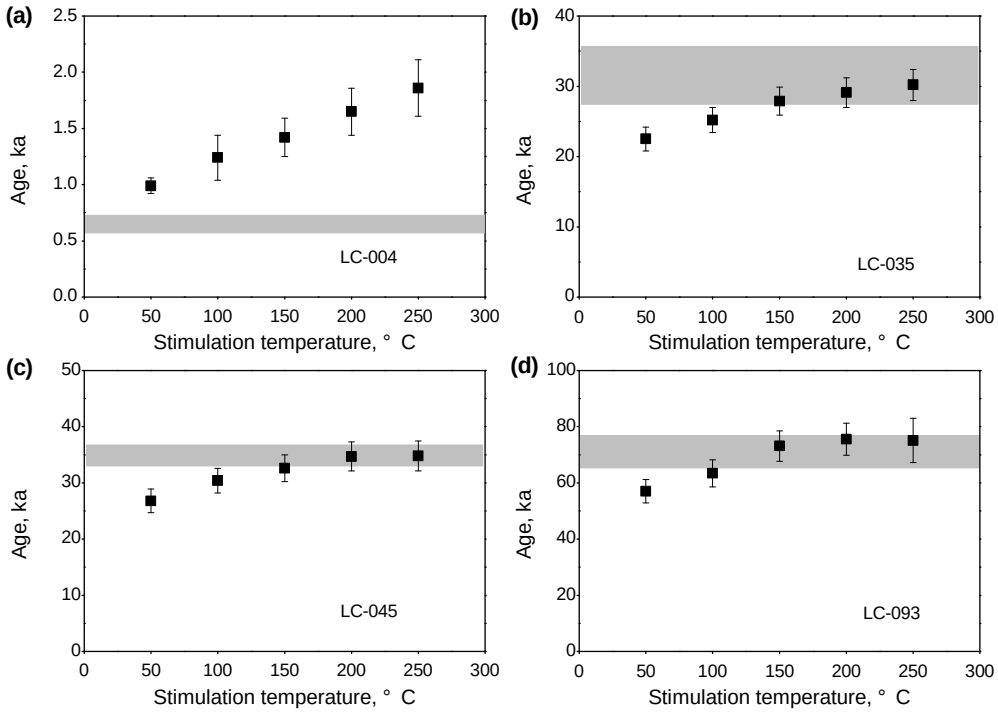
(a)
Age, ka
LC-004
Stimulation temperature, ° C
(b)
Age, ka
LC-035
Stimulation temperature, ° C
(c)
Age, ka
LC-045
Stimulation temperature, ° C
(d)
Age, ka
LC-093
Stimulation temperature, ° C

2

3

1 Fig. 3

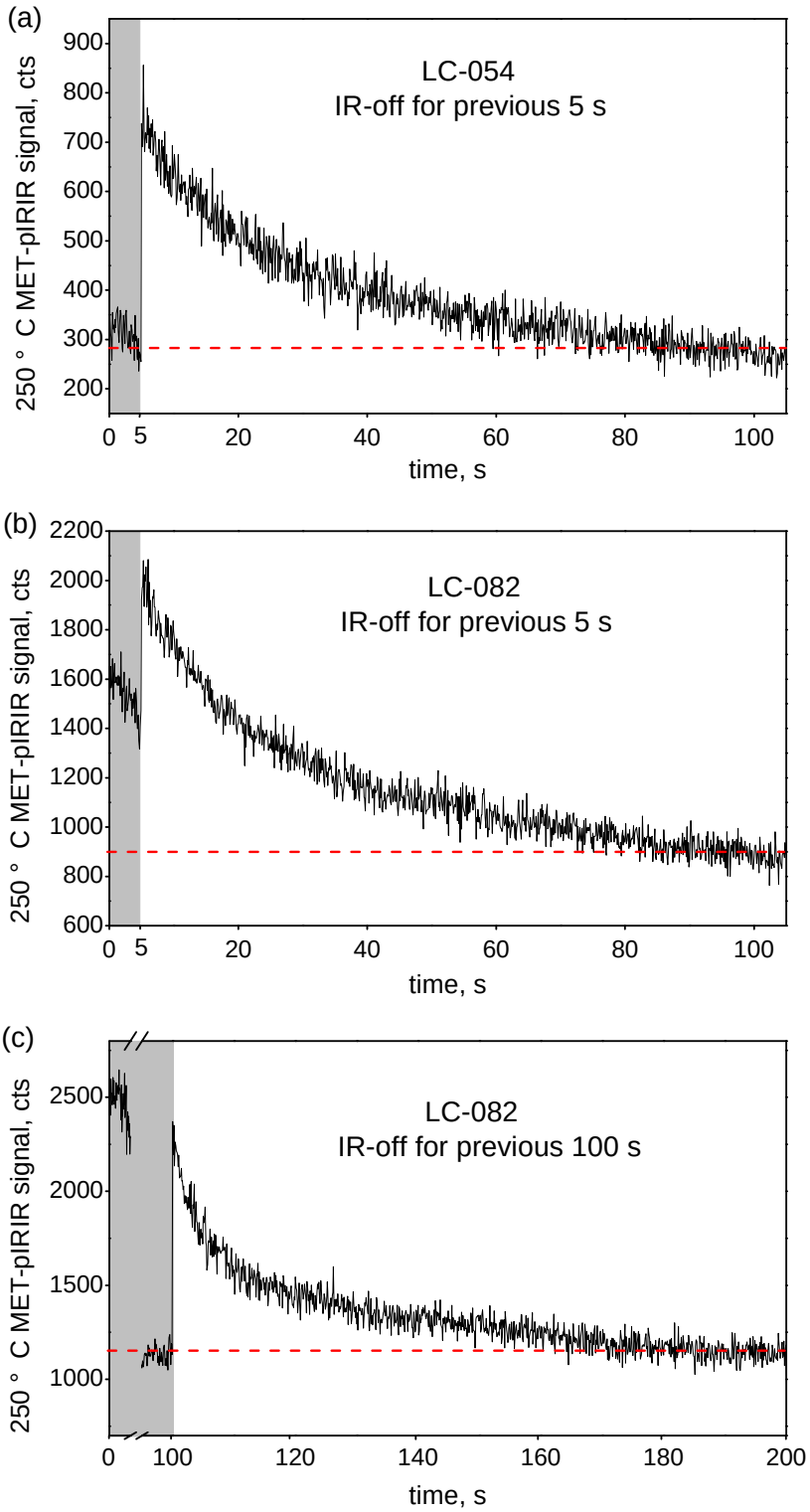
(a)
LC-054
IR-off for previous 5 s
250 ° C MET-pIRIR signal, cts
time, s
(b)
LC-082
IR-off for previous 5 s
250 ° C MET-pIRIR signal, cts
time, s
(c)
LC-082
IR-off for previous 100 s
250 ° C MET-pIRIR signal, cts
time, s

2

3

1 Fig. 4

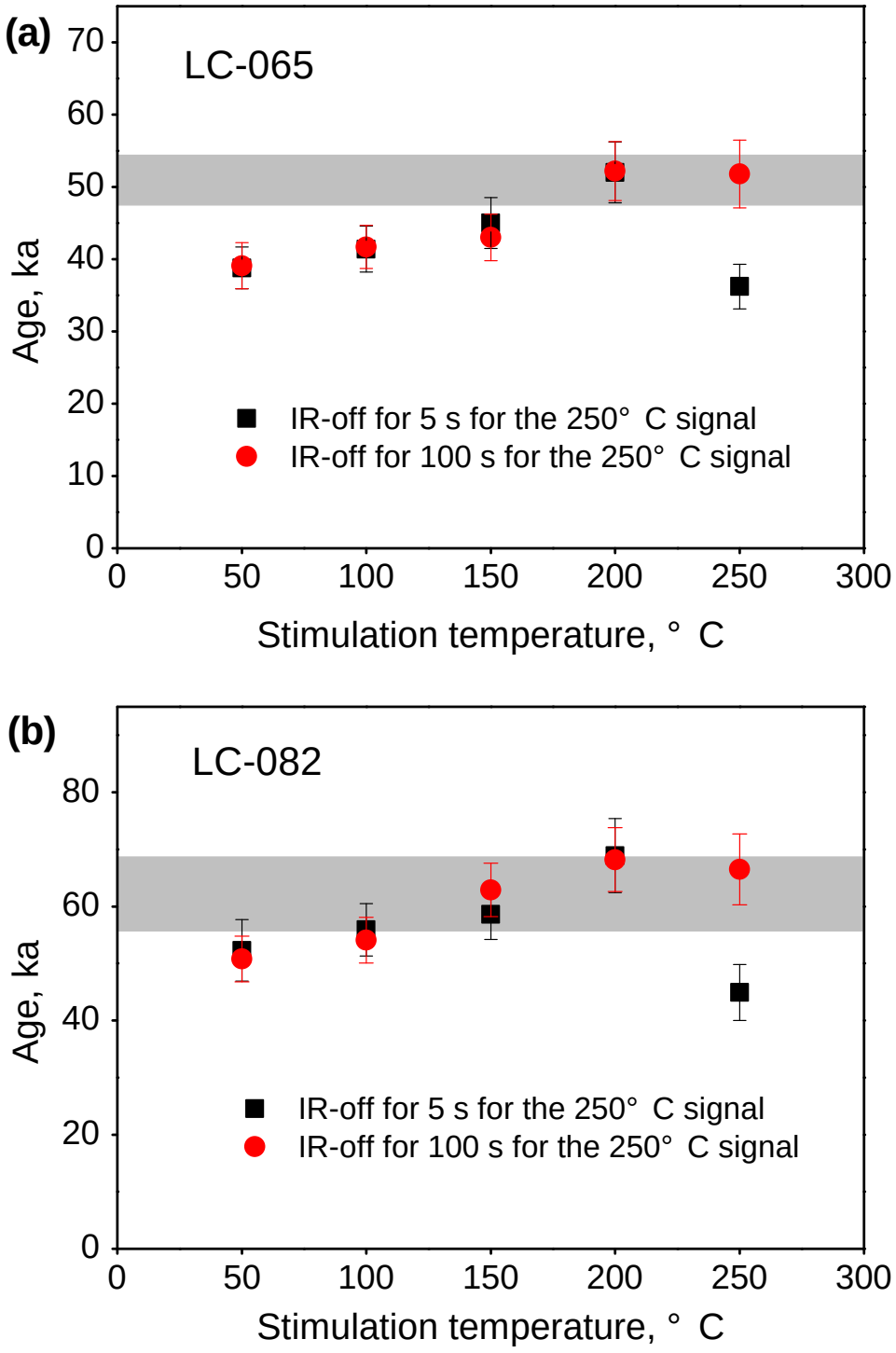
(a)
LC-065
Age, ka
Stimulation temperature, ° C
IR-off for 5 s for the 250° C signal
IR-off for 100 s for the 250° C signal
(b)
LC-082
Age, ka
Stimulation temperature, ° C
IR-off for 5 s for the 250° C signal
IR-off for 100 s for the 250° C signal

2
3

Fig. 5

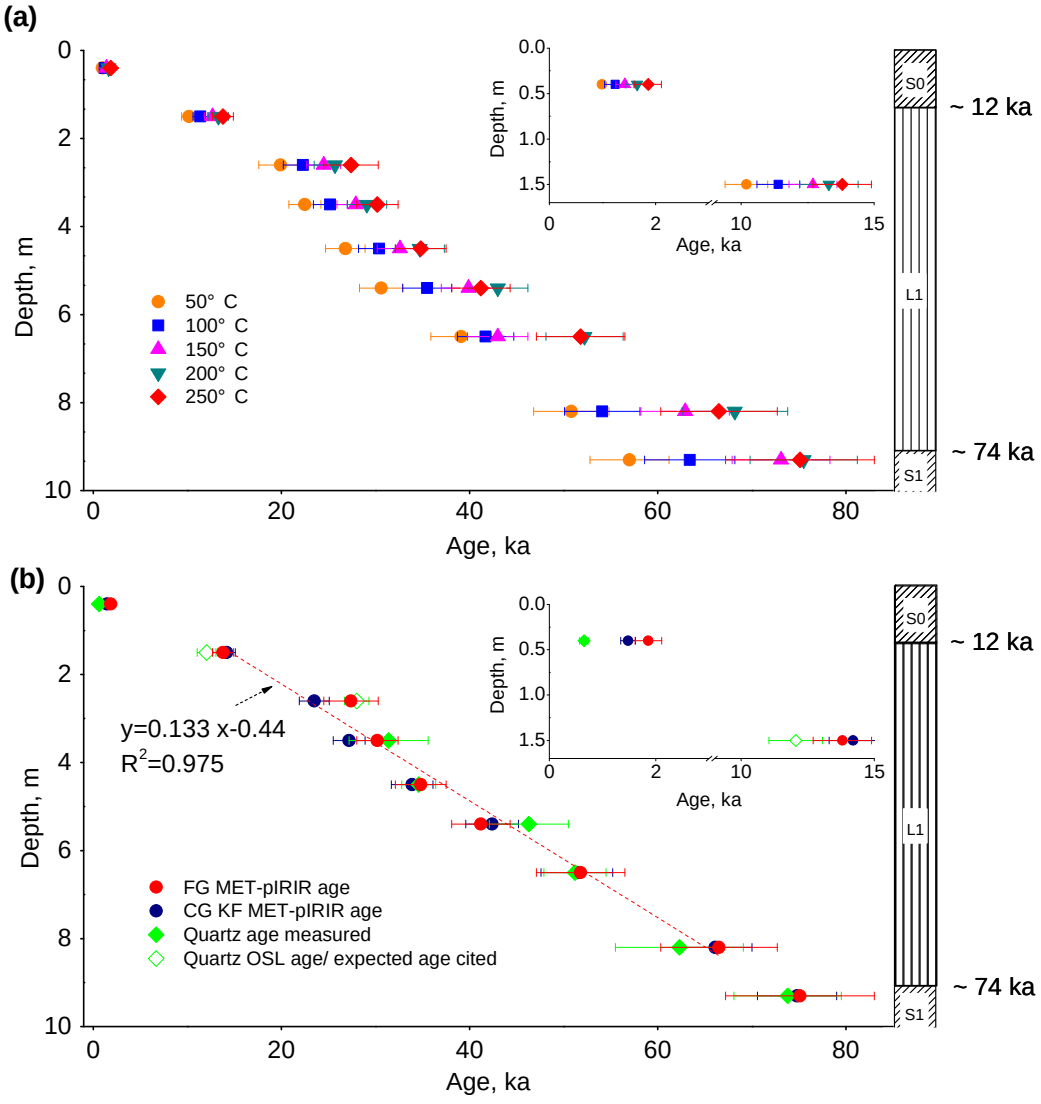
(a)
Depth, m
Age, ka
50° C
100° C
150° C
200° C
250° C
S0
L1
S1
~ 12 ka
~ 74 ka
(b)
y=0.133 x-0.44
R2=0.975
FG MET-pIRIR age
CG KF MET-pIRIR age
Quartz age measured
Quartz OSL age/ expected age cited

1 Fig. 6

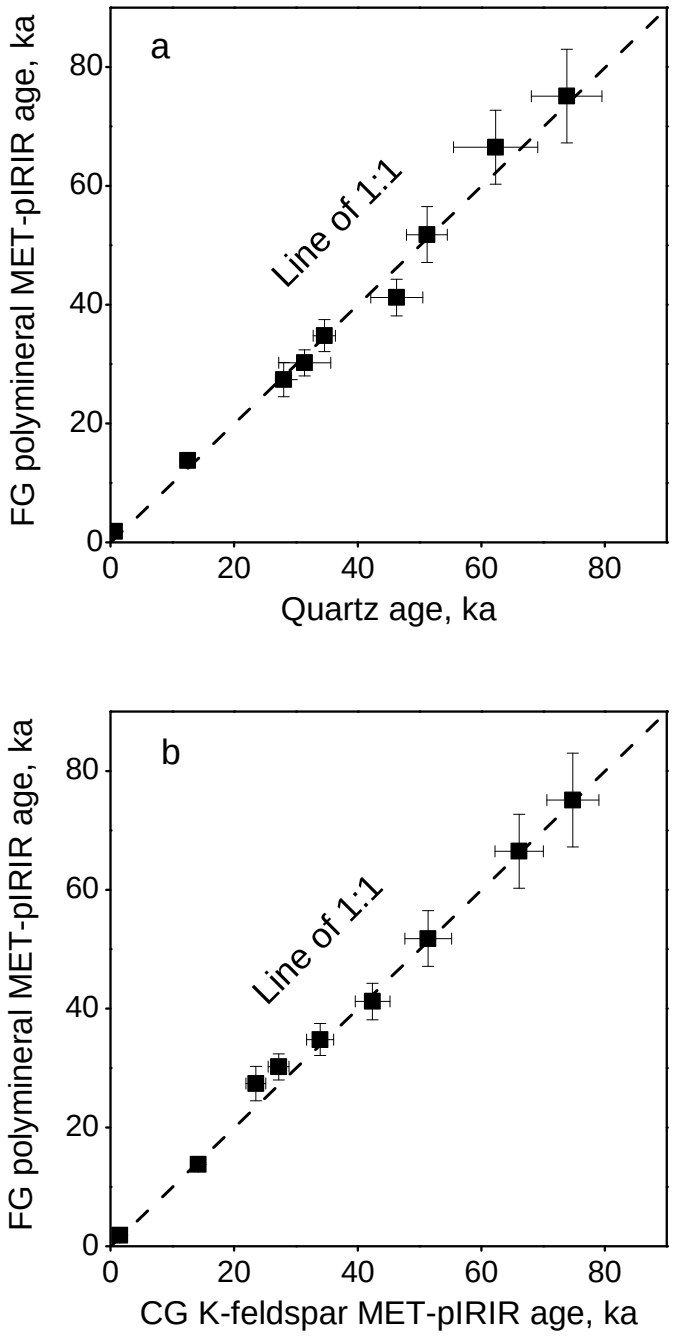
a
Line of 1:1
FG polymineral MET-pIRIR age, ka
Quartz age, ka
0
20
40
60
80
b
Line of 1:1
FG polymineral MET-pIRIR age, ka
CG K-feldspar MET-pIRIR age, ka

2